-Supporting Information-

The Ferroelectric-Gate Fin Microwave Acoustic Signal Processor

Faysal Hakim, Nicholas Rudawski, Troy Tharpe, Roozbeh Tabrizian*

Department of Electrical and Computer Engineering, Herbert Wertheim College of Engineering, University of Florida, Gainesville, FL 32611, USA

S1. Waveguide-Based Modeling of FGF Acoustic Resonators

Figure S1 shows the electrical equivalent circuit of the FGF acoustic resonator obtained from waveguide-based modeling[34] of elastic media present across the wave propagation direction (*i.e.*, resonator width).

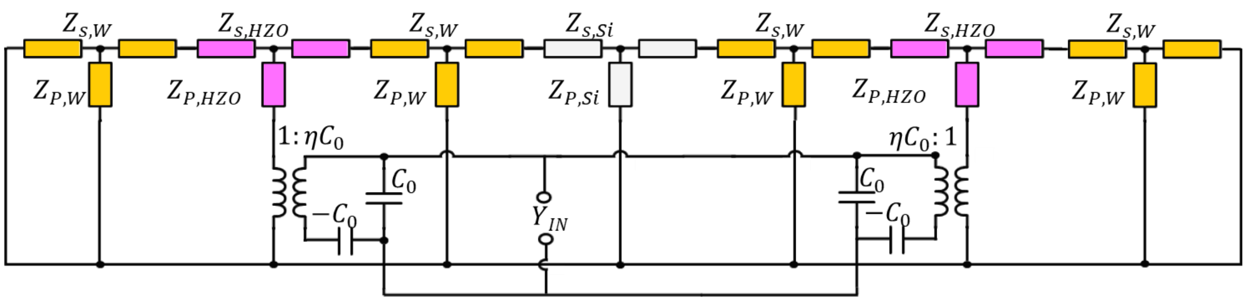

Fig. S1. Waveguide-based model of FGF resonator, enabling extraction of performance metrics for different width-extensional modes.

According to this model, any non-piezoelectric elastic medium (*i.e.*, W, Si) is represented as a T-shaped impedance network where series and shunt components are defined as:

$$Z_{P,m} = jZ_m \tan\left(\frac{k_m d_m}{2}\right)$$

$$Z_{P,m} = -\frac{jZ_m}{\sin(k_m d_m)} \quad \text{(S1).}$$

Here, k_m, d_m and Z_m are wavenumber, dimension (in wave propagation direction) and acoustic impedance of the medium. If the medium is piezoelectric (*i.e.*, HZO), then additional transformer and capacitors are added in the path of shunt impedance to represent static capacitance and transduction efficiency. The transformer turns ratio equals to $\frac{e_{33}C_0}{\epsilon}$, where e_{33}, C_0 and ε are longitudinal coupling coefficient, static capacitance per unit area, and relative permittivity of the medium. To incorporate frequency-dependent material loss (*i.e.*, finite $Q(f)$) of the medium, the wavenumber can be modified as follows: $k' = k(1 - \frac{j}{2Q(f)})$. As for dielectric loss in piezoelectric layer, a resistor can be added in series with static capacitor with value $\frac{tan\delta(f)}{2\pi f C_0}$ where $tan\delta(f)$ is the dielectric loss-tangent of the medium. Using the aforementioned formulas and parameters listed in Table S1, input admittance (*i.e.*, Y_{in}) of the FGF resonator is modeled, for varying fin width and HZO thickness, and performance metrics are extracted.

Table S1: Material properties used in waveguide-based modeling of nano fin resonators

Silicon <111>		**Ref.**
Youngs Modulus	185 GPa	35
Density	2330 kg/m^3	36
Q	15000 × freq$^{-0.15}$ + 2800	36
$Hf_{0.5}Zr_{0.5}O_2$		
Youngs Modulus	320 GPa	37
Density	7870 kg/m^3	37
Q	5e11 / freq	38
Permittivity	11 × freq$^{-0.19}$	38
e_{33}	1.5 C/m^2	Calculated from measurements
Loss Tangent	0.092 × freq$^{-0.55}$	38
Tungsten (W)		
Youngs Modulus	411 GPa	39
Density	19350 kg/m^3	39
Quality factor	5e12 / freq	40, 41
Poisson's Ratio	0.28	39

S2. Fabrication Process for FGF Acoustic Resonators and Filters

Figure S2 depicts the three-mask fabrication process flow used to implement FGF acoustic resonators and filters.

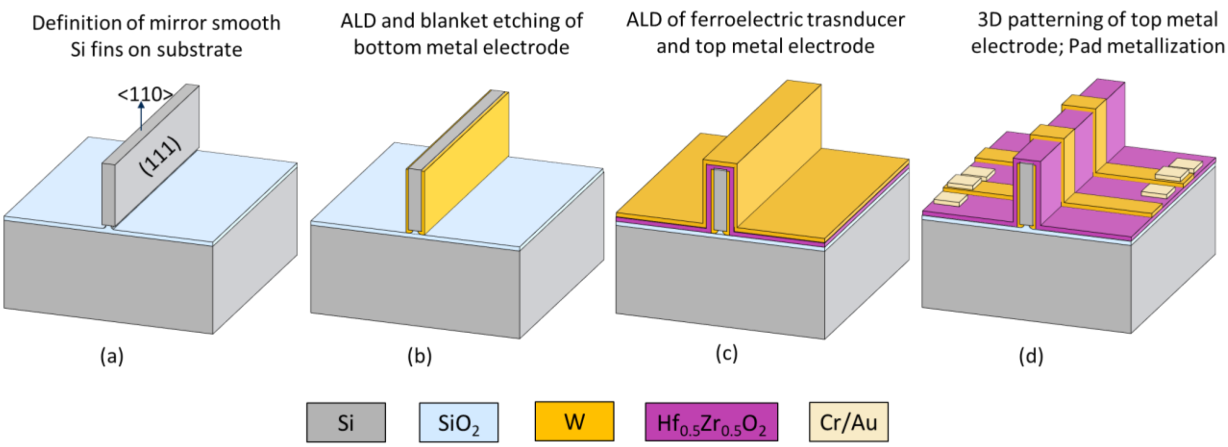

Fig. S2. Schematic of fabrication process flow for FGF resonators and filters.

Figure S3 shows perspective and top-view SEM images of devices after each key process step.

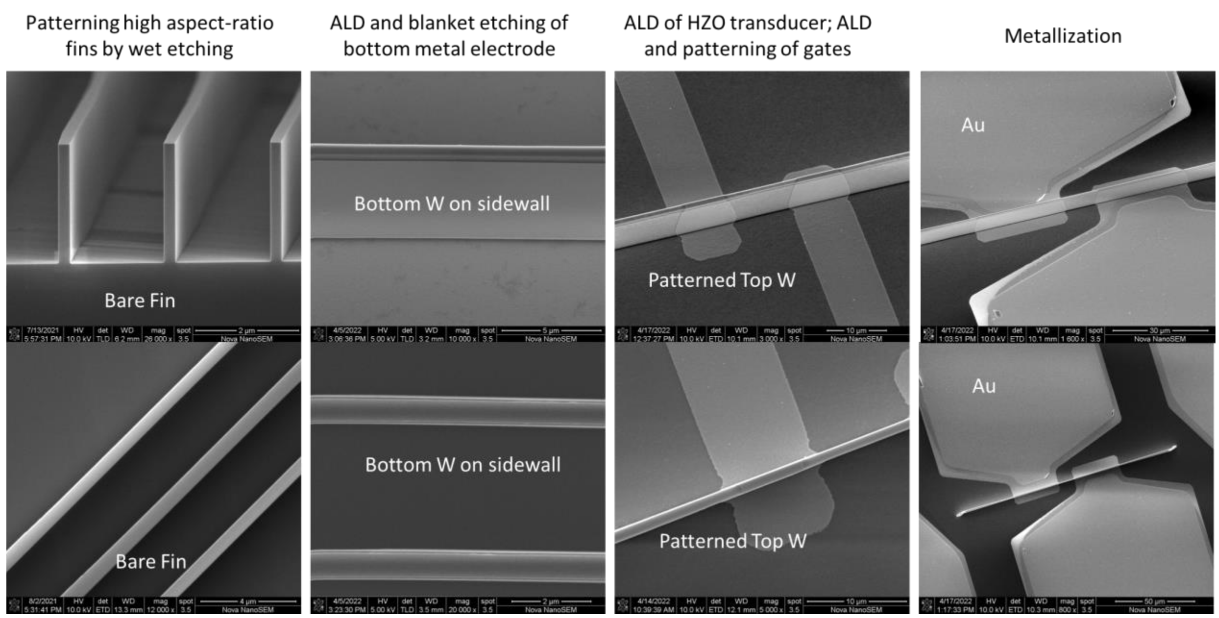

Fig. S3. Waveguide-based model of FGF resonator, enabling extraction of performance metrics for different width-extensional modes.

S3. Ferroelectric Transducer Poling

To investigate the impact of pulsed poling on superlattice $Hf_{0.5}Zr_{0.5}O_2$-Al_2O_3 transducer film, polarization hysteresis behavior of three-dimensional capacitors are measured before and after poling. Prior to poling, a soft ferroelectric behavior with small remanent polarization is evident. Figure S4 shows the polarization hysteresis loop of the 360 μm^2 three-dimensional capacitor before and after poling showing significant increase in remnant polarization from virgin state, and a hard ferroelectric behavior. The increase in remnant polarization after cycling indicates improved linear piezoelectricity and thus better electromechanical transduction in these films.

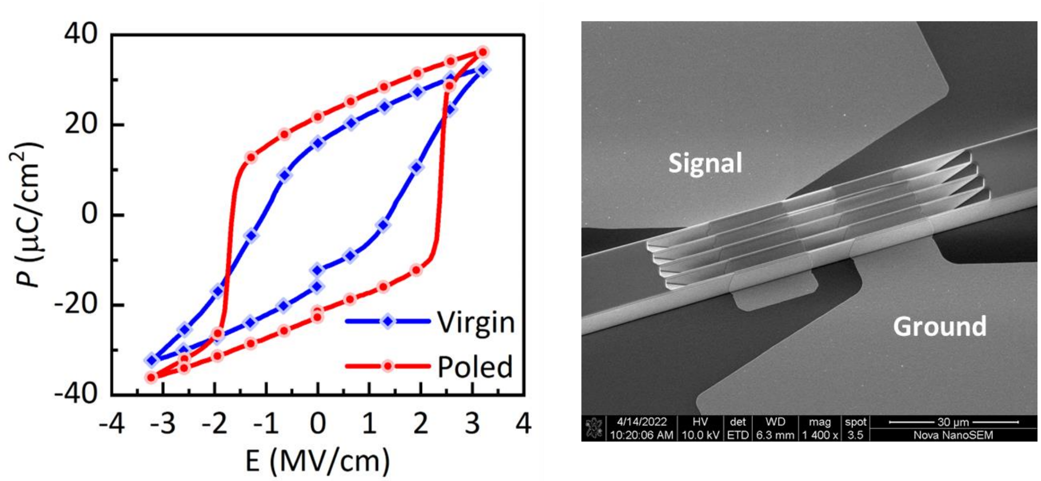

Fig. S4. Polarization hysteresis loop of an FGF before and after poling.

S4. List of Measured FGF Resonators and their Performance Merits

Table S2. Performance of WE_3 Mode

W_{fin} per design (nm)	Frequency, f (GHz)	Q	Coupling, k_t^2 (%)	$f.Q$ (10^{12} Hz)	$k_t^2.Q$	$f.Q.k_t^2$ (10^{10} Hz)
300	11.61	269	**4.94**	3.13	13.30	15.44
400	11.27	248	4.82	2.80	11.95	13.47
500	10.96	394	4.50	4.32	**17.73**	**19.43**
600	10.63	442	3.13	4.70	13.84	14.71
700	10.23	570	1.50	5.83	8.55	8.75
800	9.78	378	1.93	3.70	7.28	7.12
900	9.17	476	1.84	4.36	8.73	8.01
1000	8.55	**816**	0.46	**6.98**	3.77	3.22

Table S3. Performance of WE_1 and WE_5 Modes

Mode	W_{fin} per design (nm)	Frequency, f (GHz)	Q	Coupling, k_t^2 (%)	$f.Q$ (10^{12} Hz)	$k_t^2.Q$	$f.Q.k_t^2$ (10^{10} Hz)
WE_1	300	3.07	**1148**	0.40	3.52	4.62	1.42
WE_5		27.29	77	0.27	2.10	0.21	0.57
WE_5	400	22.73	91	0.65	2.07	0.59	1.35
WE_5	500	18.78	405	0.45	**7.60**	1.81	3.40
WE_5	900	12.42	542	**2.66**	6.73	**14.39**	**17.87**
WE_5	1000	11.86	582	2.47	6.90	14.35	17.02

S5. FGF Filter Measured Performance

Table S4: Performance of FGF Filters

Band	Series W_{fin} per design (nm)	Shunt W_{fin} per design (nm)	f_{center} (GHz)	Insertion Loss (dB)	BW_{-6dB} (MHz)	BW_{-3dB} (MHz)	Out of Band Rej. (dB)
1	850	875	9.44	8.49	157	136	-24.9 ± 0.87
2	790	830	9.73	7.58	248	95	
3	730	770	10.04	6.82	236	105	
4	640	700	10.39	6.60	272	154	
5	500	600	10.89	5.67	356	129	
6	300	400	11.51	7.68	341	187	

Reference:

[34]W. P. Mason, "Electromechanical Transducers and Wave Filters," 2nd Edition, Van Bistrabd D. Company Inc., New York, 1948.

[35]Accessed on: October 20, 2021: http://www.ioffe.ru/SVA/NSM/Semicond/Si/

[36]R. Tabrizian, M. Rais-Zadeh and F. Ayazi, "Effect of phonon interactions on limiting the f.Q product of micromechanical resonators," *TRANSDUCERS 2009 - 2009 International Solid-State Sensors, Actuators and Microsystems Conference*, Denver, CO, USA, 2009, pp. 2131-2134, doi: 10.1109/SENSOR.2009.5285627.

[37]T. Tharpe, X. Zheng, P.X. Feng, and R. Tabrizian, "Resolving Mechanical Properties and Morphology Evolution of Free-Standing Ferroelectric $Hf_{0.5}Zr_{0.5}O_2$.," *Advanced Engineering Materials*, 2021, doi: 10.1002/adem.202101221.

[38]M. Dragoman, M. Aldrigo, D. Dragoman, S. Iordanescu, A. Dinescu, M. Modreanu, “HfO2-Based Ferroelectric Applications in Nannoelectronics”, *in Physica Status Solidi Rapid Research Letters*, 2021, doi:10.1002/pssr.202000521.

[39]ASM Metals Reference Book, Third edition, Michael Bauccio, Ed. ASM International, Materials Park, OH, 1993.

[40]J. A. Rayne and D. P. Almond, "Temperature Dependence of Electron Mean Free Path in Molybdenum and Tungsten from Ultrasonic Measurements," *1976 Ultrasonics Symposium*, 1976, pp. 638-641, doi: 10.1109/ULTSYM.1976.196759.

[41]W. Duffy Jr., “Acoustic quality factor of molybdenum and tungsten at low temperatures”, *Journal of Applied Physics* **72**, 5628 (1992); doi:10.1063/1.352324